Atmospheric Research 268 (2022) 105981

Contents lists available at ScienceDirect

Atmospheric Research

journal homepage: www.elsevier.com/locate/atmosres

Initiation of lightning flashes simultaneously observed from space and the ground: Narrow bipolar events

Jesús A. López [a,*], Joan Montanyà [a], Oscar van der Velde [a], David Romero [a], Francisco J. Gordillo-Vázquez [b], Francisco J. Pérez-Invernón [c], Alejandro Luque [b], Carlos Augusto Morales Rodriguez [d], Torsten Neubert [e], William Rison [f], Paul Krehbiel [f], Javier Navarro González [g], Nikolai Østgaard [h], Víctor Reglero [g]

[a] Lightning Research Group, Technical University of Catalonia, Edifici TR1, Carrer Colom 1, Terrassa 08222, Spain
[b] Instituto de Astrofísica de Andalucía, CSIC, Glorieta de la Astronomia s/n, Granada, Spain
[c] Deutsches Zentrum für Luft- und Raumfahrt, Institut für Physik der Atmosphäre, Weßling, Germany
[d] Departamento de Ciências Atmosféricas, Instituto de Astronomia, Geofísica e Ciências Atmosféricas, Universidade de São Paulo, São Paulo, Brazil
[e] National Space Institute, Technical University of Denmark (DTU Space), Kongens Lyngby, Denmark
[f] Langmuir Laboratory for Atmospheric Research, Geophysical Research Center, New Mexico Institute of Mining and Technology, Socorro, NM 87801, USA
[g] Image Processing Laboratory, University of Valencia, Valencia, Spain
[h] Birkeland Centre for Space Science, Dept. of Physics and Technology, University of Bergen, Bergen 19, Norway

A B S T R A C T

We investigate the initiation of four lightning flashes detected from ground by means of the Colombia Lightning Mapping Array (Colombia-LMA) and simultaneously observed from space by the optical sensors of the Atmosphere-Space Interactions Monitor (ASIM) on board the International Space Station (ISS), the Geostationary Lightning Mapper (GLM), and the Lightning Imaging Sensor on the ISS. The initiations of the flashes are characterized by isolated and predominant optical blue pulses (337.0 nm). In three of the flashes, red emissions (777.4 nm), a dominant line of hot lightning, were not detected during their initiation. In these cases, the initiations were also accompanied by bipolar VLF/LF waveform with a narrow short duration (<40 μs) and VHF emissions with high radio frequency power (<269 kW). The detection of the blue emissions without any red luminosity supports that the fast breakdown processes at the flash initiation can be exclusively of streamer nature. The onset of the fourth flash was associated with both blue and red radiation, and with weak narrow bipolar waveform in VLF/LF and low VHF power. The flashes initiated between the midlevel negative and upper positive charge regions. This paper presents and discusses the first fast breakdown processes observed simultaneously from ground by means a Lightning Mapping Array (LMA) and from space during the onset of lightning flashes.

1. Introduction

Much is still unknown about the initiation of lightning. Despite the fact that the electricity associated with thunderstorms and lightning has been studied since the 17th century, as of today, the exact mechanisms of initiation of lightning flashes remain insufficiently understood. It is well known that non-thermal streamer discharges are primarily required for the formation of hot leader channels (e.g. Bazelyan and Raizer, 1997). In lightning, the leader discharge allows the extension of the channels covering distances of several tens of kilometers (e.g. van der Velde and Montanyà, 2013). It has recently been evidenced by Rison et al. (2016) that the initiation of lightning flashes might be associated with extensive streamer intracloud corona (ICC) discharges that produce intense Very High Frequency (VHF) power pulses with associated radio sferics (narrow bipolar events or NBEs). The simultaneous occurrence of powerful VHF emissions and NBEs related to in-cloud processes are known as compact intracloud discharges (CIDs) and were first reported by Le Vine (1980) and described in detail by Eack (2004), Jacobson et al. (2013), Lu et al. (2011) and Liu et al. (2019), among many other works.

Several recent studies have used high-resolution lightning mapping systems such as VHF broadband digital interferometers and Lightning Mapping Arrays (LMAs) to investigate the occurrence and propagation of electric breakdown at the initiation of lightning flashes. Rison et al. (2016) showed that the initiation of intracloud (IC) and cloud-to-ground (CG) lightning discharges often exhibited powerful VHF emission associated with NBEs, consistent with radiation from fast positive breakdown processes (FPB) of streamer nature. A similar study by Kolmašová et al. (2018) correlated measurements of VHF radio emissions by an LMA with a sequence of preliminary breakdown pulses of IC and CG lightning flashes obtained from a broad-band magnetic field

* Corresponding author.
E-mail address: jesus.alberto.lopez@upc.edu (J.A. López).

https://doi.org/10.1016/j.atmosres.2021.105981
Received 7 August 2021; Received in revised form 12 November 2021; Accepted 14 December 2021
Available online 20 December 2021

measurements. In that study, strong VHF radio power emissions were mainly matched with the first preliminary breakdown pulse. Tilles et al. (2019), reported the occurrence of fast negative breakdown (FNB) processes during the initiation of lightning flashes which were also associated with NBEs. In addition, by using a high-speed VHF radio interferometer, Lyu et al. (2019) showed that fast positive breakdown processes can initiate some, but not all, lightning flashes. In the same year, Marshall et al. (2019) expanded the study of the initial breakdown pulses (IB pulses) as an essential factor for the initiation of IC and CG flashes. These authors found that the initial electric field changes of IB pulses were associated with short VHF broadband pulses mainly attributed to positive corona streamers. More recently, Bandara et al. (2020) showed, that in some cases, NBEs do not necessarily report a large radio power emission to initiate an IC discharge, which is consistent with results previously reported by Lyu et al. (2019). These recent findings suggest that the initiation of IC or CG discharges may be associated with VHF power radiation from breakdown processes of corona streamer discharges, which can also be the source of strong VHF radiation as in the case of NBEs.

Up to now there is no optical evidence of the streamer nature of the fast breakdown at the onset of lightning. In this sense, Soler et al. (2020) using observations from the Atmosphere-Space Interactions Monitor (ASIM) (Neubert et al., 2019), has associated strong sferics radio bursts to blue (337.0 nm) optical emissions from lightning. These emissions are assumed to be produced by streamer corona discharges in thunderclouds, whose nighttime climatology, global geographical and seasonal distributions have been recently published (Soler et al., 2021). Results from Soler et al., 2021 indicate that the northwest region of Colombia is the region of the world with most cloud corona discharges. Finally, it has been also suggested that fast streamer breakdown may be also related with the occurrence of TGF (Tilles et al., 2020).

In this paper we report the initiation of four lightning flashes simultaneously observed by the Colombia-LMA and the photometers of ASIM-MMIA. The paper is organized as follows. The data is introduced in the next section. In section three, the initiations of the four lightning flashes are described by means of the LMA and the optical detections by ASIM. The occurrence of the fast breakdown in the electrical charge structure is determined and the sferics of the NBE presented. Section four contains the discussion and the paper ends with the conclusions.

2. Data

Locations of VHF sources from lightning are provided by the Colombia-LMA. This network has been operational since 2015 as part of the ground support for the ASIM mission in the tropics (López et al., 2019). Since June 2018, the Colombia-LMA operated at the Magdalena River Valley in the center of Colombia including 8 stations. Each station has a VHF receiver tuned at the frequency range between 60 and 66 MHz. Baselines between stations range from 7 to 25 km around Barrancabermeja city (Fig. 1). The LMA detects and locates sources of VHF emissions produced by electrical breakdown processes (Rison et al., 1999). Radio frequency power at the LMA frequencies is determined for each detected source. More information about the LMA and its performance can be found in Rison et al., 1999 and Thomas et al., 2004.

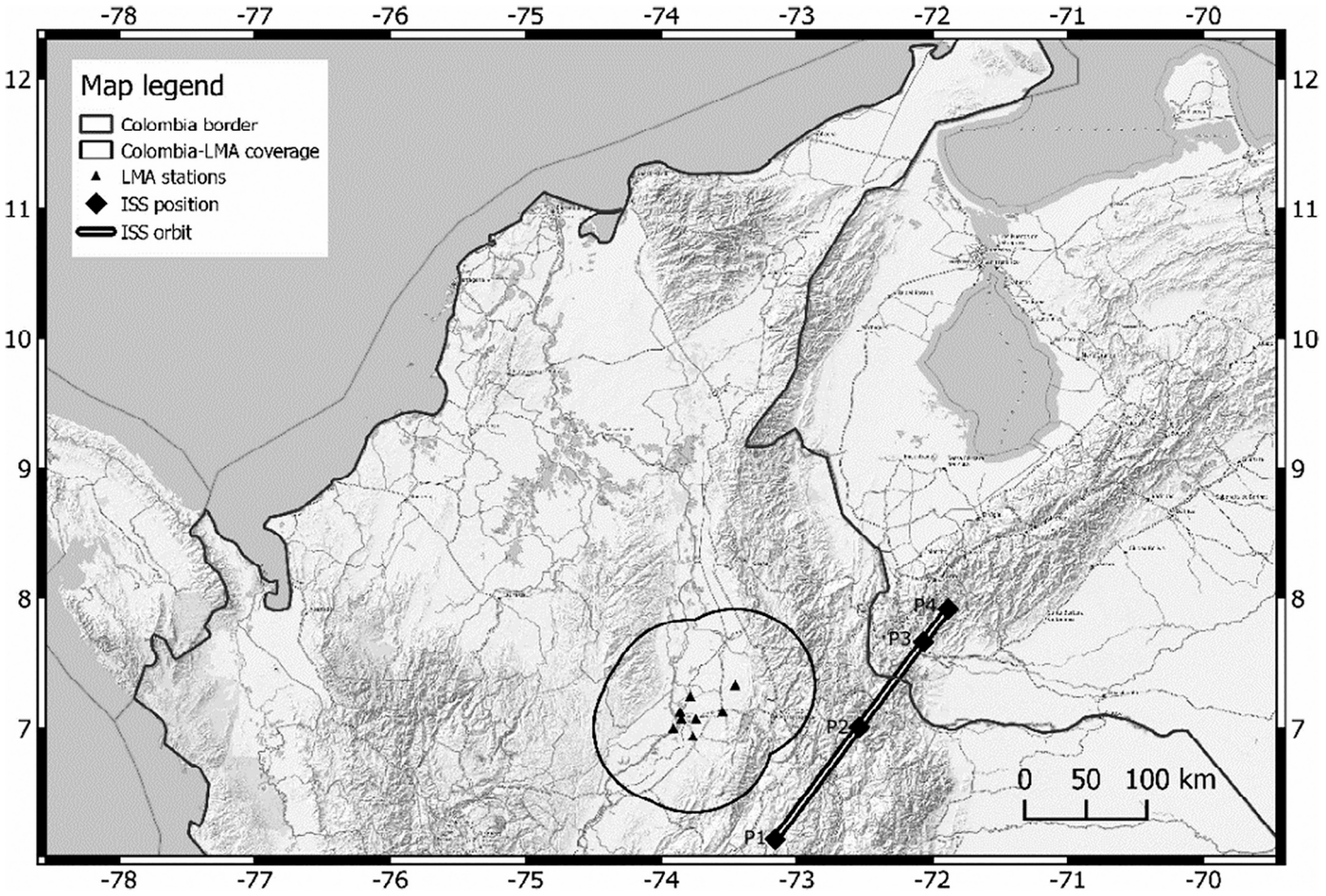

Fig. 1. Geographical location of the Colombia-LMA network. Each triangle represents an LMA receiver around Barrancabermeja city. The high-efficiency coverage area is approximated by a buffer of 65 km. In the same figure, the positions of the ISS (black diamonds) are plotted at the time of each detected LMA flash. P1-P4 labels correspond to the ISS-LIS location at the time of each LMA flash.

Detections of VLF/LF emissions from total lightning flashes (IC and CG) are supplied by the national VLF/LF LINET lightning detection system in Colombia (Betz et al., 2009; Aranguren et al., 2017). LINET-Colombia is composed of 21 radio receivers (VLF/LF) with baselines from 100 km to 200 km (Aranguren et al., 2017). In addition, we have also considered lightning stroke information from the Global Lightning Detection network (GLD360) (Said et al., 2013). Finally, magnetic field waveforms (5–200 kHz) for each of the analyzed lightning flashes are included in this study.

Optical emissions at the initiation of the investigated flashes are obtained from three space-based optical instruments. The primary instrument is the Modular Multispectral Imaging (MMIA) instrument on the ASIM (Chanrion et al., 2019) on board the International Space Station (ISS). MMIA is composed of an array of three photometers and two cameras. The three photometers observe in the 180–250 nm, 337.0 nm (±4 nm) and 777.4 nm (±5 nm) spectral bands at a sample rate of 100 kHz. The two cameras are one-megapixel recording 12 frames per second with spectral bands centered at 337.0 nm (±5 nm) and 777.4 nm (±3 nm). In addition to ASIM, optical information from two space-based lightning imagers is included. These lightning imagers measure narrowband, near-infrared optical emissions at 777.4 nm produced by excited atomic oxygen radiative emissions from lightning. One of these instruments is the Geostationary Lightning Mapper (GLM) on the Geostationary Operational Environment Satellites (GOES) 16 and 17, launched in 2016 and 2018 respectively. GLM is the first geostationary instrument dedicated to the continuous monitoring of intracloud and cloud-to-ground lightning. The instruments monitor the Americas with a temporal resolution of 2 ms, a bandwidth of 1 nm and a spatial accuracy at satellite nadir of about 8 km (Goodman et al., 2008; Goodman et al., 2013). The other instrument is the Lightning Imaging Sensor on the ISS (ISS-LIS) (e.g. Blakeslee et al., 2020). ISS-LIS has a pixel position accuracy <4 km and an image sample rate of 2 ms. For each elementary detection (called events), the GLM and ISS-LIS provide the optical radiance. In the following, we use "red" for 777.4 nm band (ASIM-MMIA, GLM and ISS-LIS) and "blue" for the 337.0 nm band (only ASIM-MMIA). Finally, the time accuracy of the ASIM photometers was sequentially improved mainly by aligning the highest irradiances reported by GLM, ISS-LIS and MMIA-ASIM (analyzing the photometers centered at the 777.4 nm band) and by the GPS time of the corresponding ground-based detections of lightning strokes.

3. Results

3.1. General overview

On 30 October 2019, a total of 20 lightning flashes were simultaneously observed from ground by the Colombia-LMA and from space by ASIM, GLM and ISS-LIS. Out of the 20 flashes, four exhibited clear isolated optical pulses during their initiations detected mostly by the blue ASIM photometer, alongside intense VHF power emissions. All these flashes were produced in a secondary small convective cluster of a multicell thunderstorm system located in the Magdalena River Valley to the

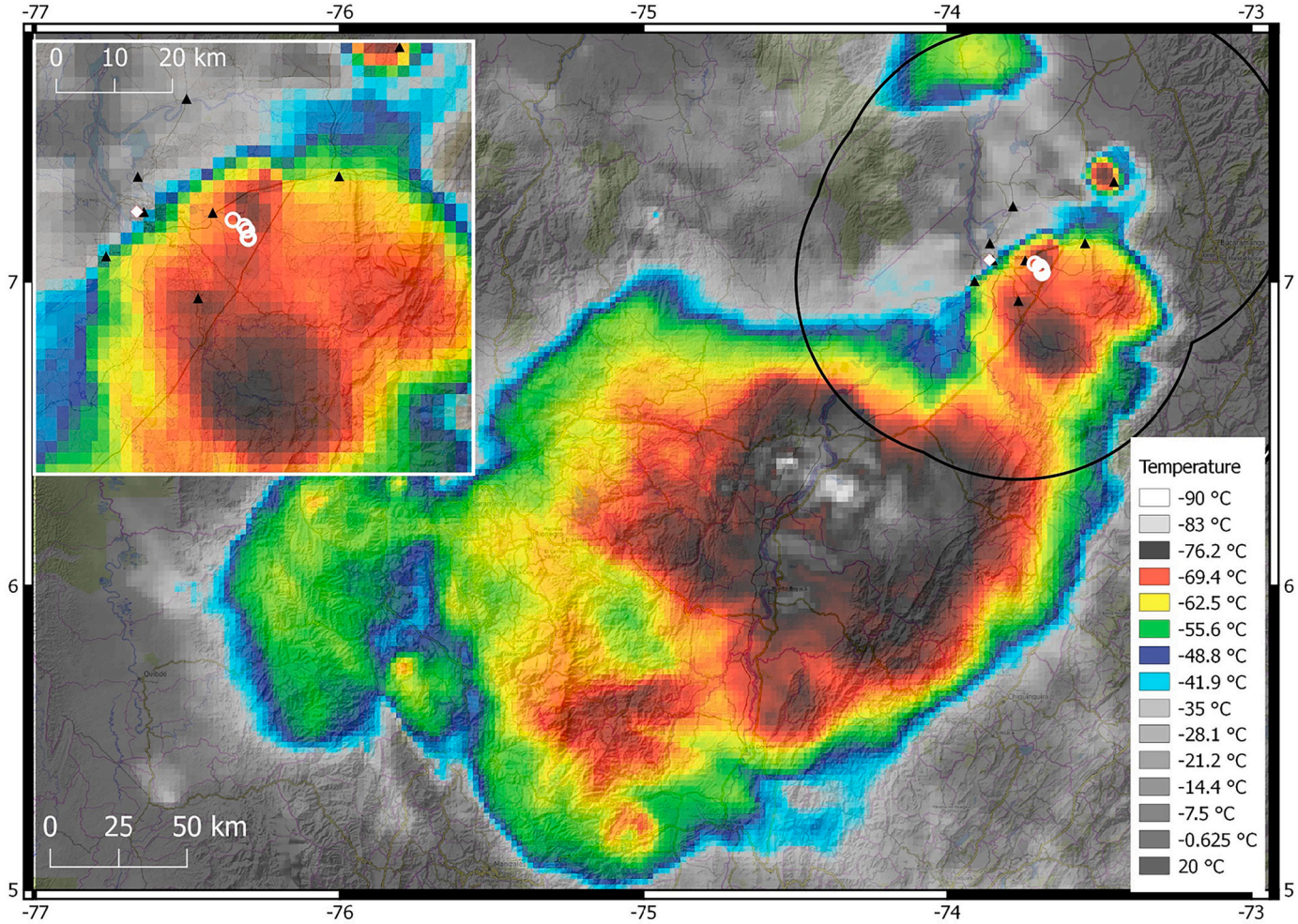

Fig. 2. Cloud top temperature of the thunderstorm associated with the four investigated lightning flashes. White circle markers correspond to the first detected VHF source of each flash whereas the white diamond is the location of the magnetic sensor and the black triangles are the LMA stations.

southwest of Barrancabermeja (7°15′N; 73°34′W) (see Fig. 2). The four flashes occurred at 06:05 in the seconds 11; 28; 41 and 46 UTC, respectively. The range of the cloud top temperatures around the initiation area of the four flashes was between −69 °C and − 76 °C, according to GOES-16 infrared cloud measurements (white circle markers in Fig. 2), with corresponding altitudes between 14 and 15 km, as inferred from the nearest balloon sounding. The height of the tropopause was approximately 17.5 km according to the sounding.

3.2. Cloud irradiance energy and lightning VHF power emissions

Figs. 3 to 6 show the temporal evolution of the optical and VHF signals associated with each one of the four analyzed flashes. In these figures, panel (a) displays the LMA VHF power for each of the detected sources. Panels (b) and (c) are the optical blue and red photometric light signals recorded by ASIM-MMIA, respectively. In these plots, the 100 kHz photometer signals have been smoothed by a 10-sample moving average. Panel (d) depicts the cloud energy of the 777.4 nm optical emissions recorded by the GLM and ISS-LIS, binned at the interval of every two milliseconds.

The first flash (Fig. 3a) initiated with the strongest VHF power emission of the entire flash. The power was estimated to be 52.5 dBW (~178 kW). This was accompanied by an isolated optical blue pulse (Fig. 3b) with no simultaneous detection in the red (Fig. 3c). One can deduce a rise time of this blue pulse of about 380 μs lasting ~2.3 ms similar to those reported by Soler et al. (2020). At the same time, a stroke by LINET and GLD360 was detected at the time of the first LMA source and at the rise of the blue optical pulse (see dot and triangle markers in Fig. 3). After the initiation, the rest of the detected blue emissions had a coincident red signal (e.g. see the negative CG stroke produced 259 ms after). At this time, blue and red signals presented high amplitudes but accompanied with much lower VHF power. Note that the detections of GLM and ISS-LIS in Fig. 3d match well with the ASIM red channel signals in Fig. 3c with higher amplitudes as also reported before by van der Velde et al. (2020).

The second flash (Fig. 4) produced the strongest VHF power emission among the other flashes. This emission occurred at the onset of the flash (Fig. 4a) with an amplitude around 54.3 dBW (~269 kW). The initiation of this flash was again characterized by an isolated blue emission (Fig. 4b). The blue optical pulse exhibited a rise time of about 200 μs and lasted for about 3.3 ms. There were no detections of concurrent red optical emissions during the initiation of this event, as can be seen in Fig. 4c–d. As in the previous flash, a stroke was detected by the GLD360 at the time of the initiation. This stroke was detected only 31 μs after the first LMA source and was classified as CG. Three additional strokes were later detected by LINET during the flash, two of which were classified as IC discharges and one as CG, as shown in Fig. 4 (see points and cross markers).

The third flash (Fig. 5) also initiated with VHF emission. In this case, the power level was lower than the former cases with about 40 dBW (~10 kW), see Fig. 5a. This initial VHF source was accompanied by an isolated blue optical pulse (500 μs rise time and 3 ms duration) with no detection of red emissions (see Fig. 5c-d). After the first VHF source, there was a gap of about 27 ms without LMA VHF sources. After this period, a series of VHF radiation bursts located at slightly higher altitude (>12.5 km) were almost always accompanied by frequent pulses of blue light (and very weak red emissions) during two relatively long periods of time lasting for about 90 ms and 30 ms at the beginning and at the end of the flash, respectively. We speculate that the previously described sequence of VHF-blue, radio-optical pulses could be a distinct manifestation of sequence of cloud corona discharges that occur near the upper boundary of the upper positive layer (see Fig. 7) growing as an negative leader through the positive layer. It is worth mentioning that the amplitude of the first blue optical pulse, likely from fast breakdown, is roughly twice the amplitude of each of the more than 10 subsequent blue pulses in the supposed cloud corona discharge. The assumption of the cloud corona activity is supported by the limited red optical emissions. Additionally, the highest detected blue and red optical pulses that

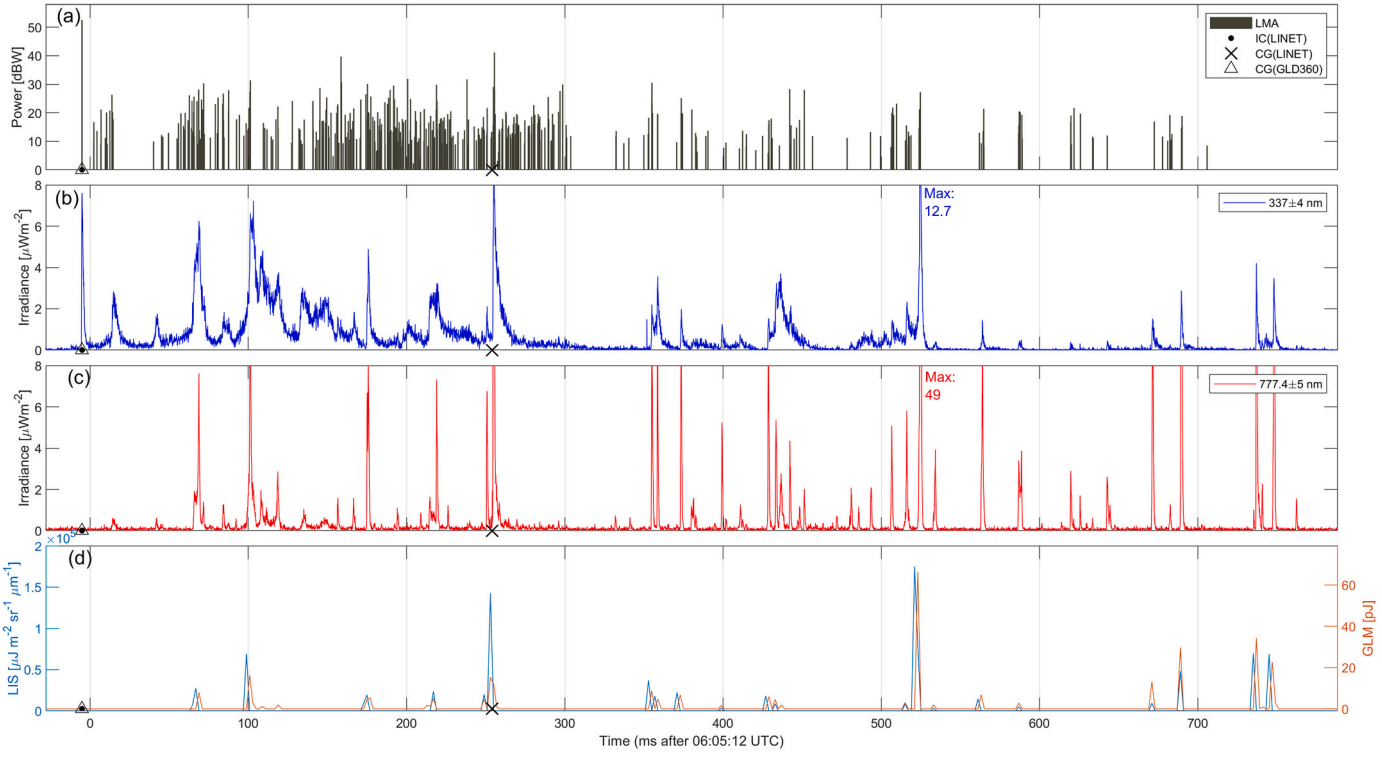

Fig. 3. VHF RF power and optical luminosity of the first lightning flash at 06:05:11. Panel (a) shows the LMA VHF RF power for each of the detected sources. Panels (b-c) are the optical radiances for the 337.0 nm (blue) and 777.4 nm (red) luminosity from the MMIA-ASIM photometers. Panel (d) shows the optical energy from ISS-LIS and GLM at 777.0 nm (red). (For interpretation of the references to colour in this figure legend, the reader is referred to the web version of this article.)

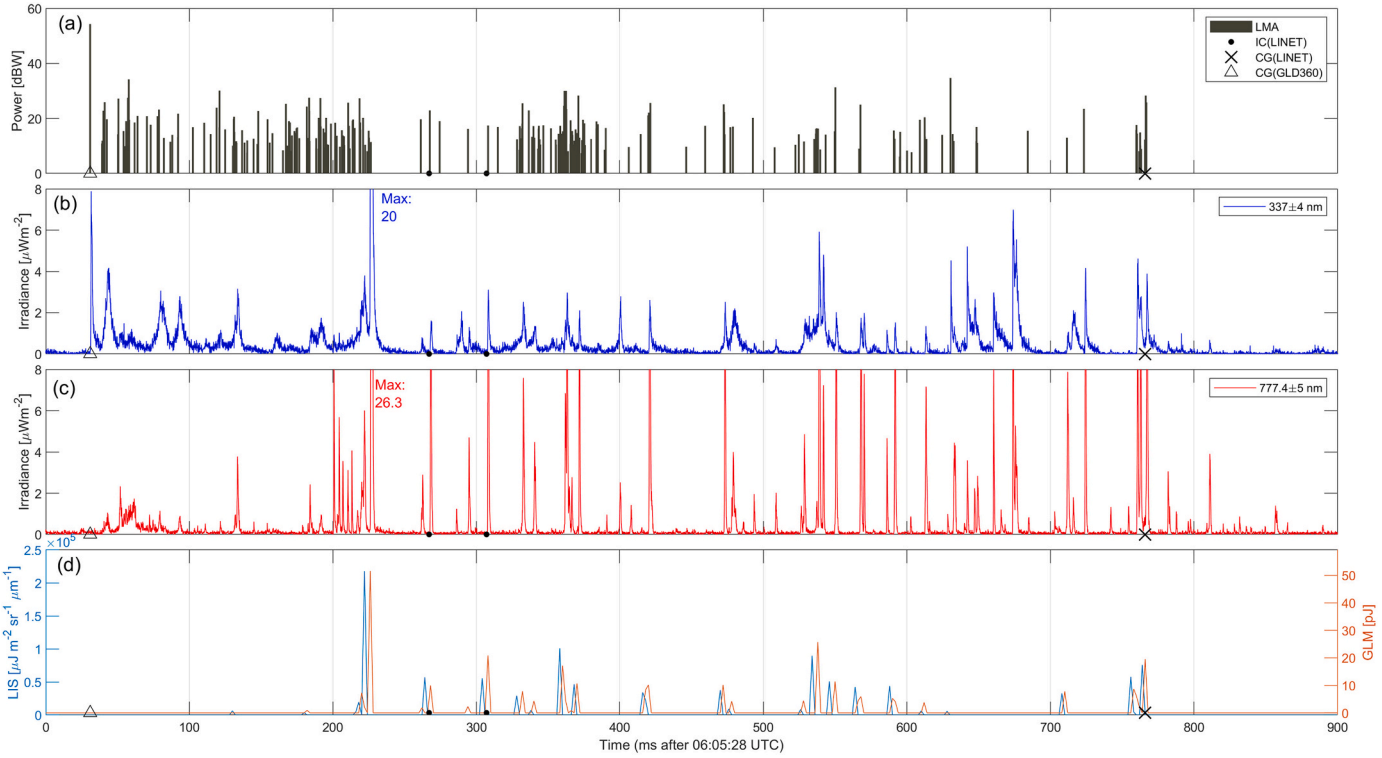

Fig. 4. VHF RF power and optical luminosity of the second lightning flash at 06:05:28. Refer to Fig. 3 for the description of the panel.

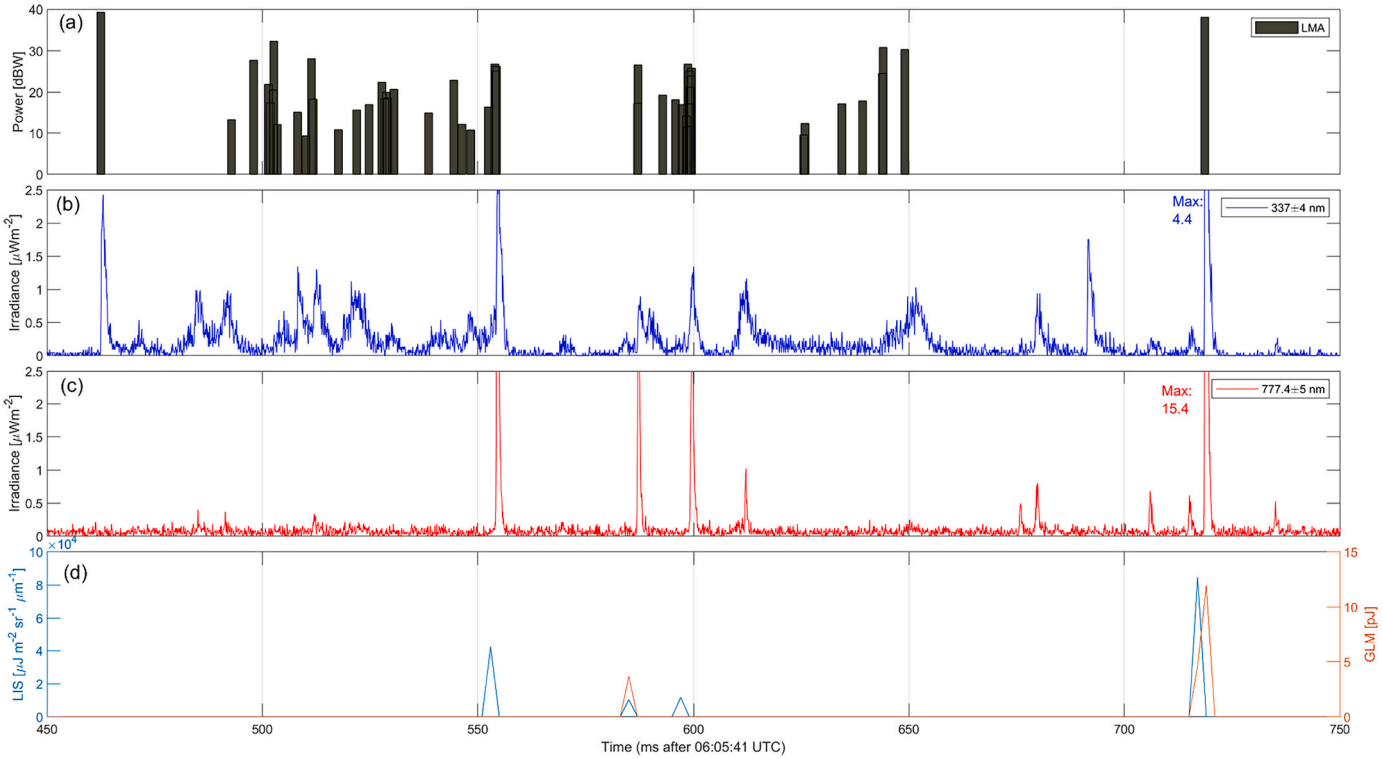

Fig. 5. VHF RF power and optical luminosity of the third lightning flash at 06:05:41. Refer to Fig. 3 for the description of the panel.

occurred near the end of the flash were accompanied by an intense VHF source of 38.9 dBW (~7.7 kW).

The VHF power emitted at the onset of the last flash (Fig. 6) was the smallest and around 20 dBW (~100 W), as is shown in Fig. 6a. The bright optical emission during the initiation of this flash was dominated by a blue pulse (Fig. 6b) alongside a weaker red emission (Fig. 6c). The rise time and duration of the first and isolated blue pulse are calculated resulting 392 μs and 2.7 ms, respectively. Additionally, there were no detections (strokes) by the lightning location systems associated to the beginning of the flash.

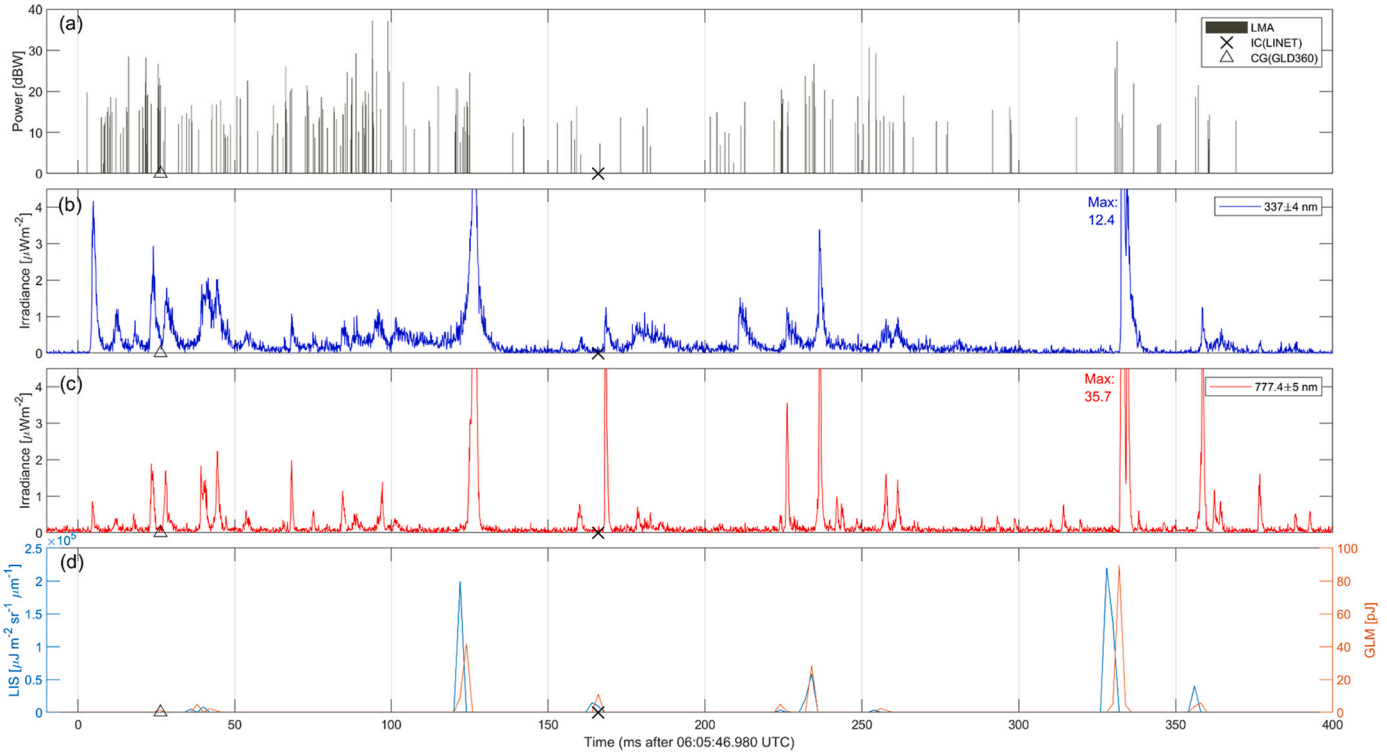

Fig. 6. VHF RF power and optical luminosity of the fourth lightning flash at 06:05:46. Refer to Fig. 3 for the description of the panel.

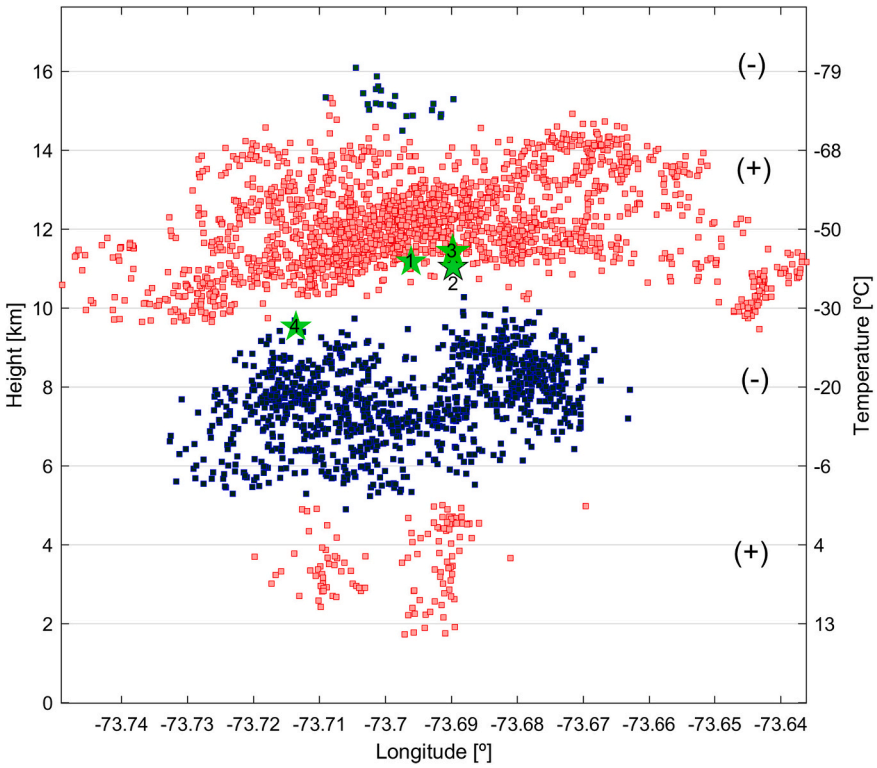

Fig. 7. Charge structure during an interval of 10 min derived from the identified polarity of the LMA sources. Red and blue colors correspond to the positive and negative polarity of the charge layers, respectively. A small negative charge screening layer is detected between 15 km and 16 km. Star markers are the locations of the flash initiations (numbers correspond to the flash identification). (For interpretation of the references to colour in this figure legend, the reader is referred to the web version of this article.)

3.3. Range heights of the studied flashes and thunderstorm charge structure

Using the identification of the polarity of lightning leaders (van der Velde and Montanyà, 2013) and the vertical propagation of the initial sources (López et al., 2019), the electrical charge structure of the thunderstorm during the period of the investigated flashes is determined. Applying this methodology, we find that the storm exhibited a tripolar charge structure as can be seen in Fig. 7. The upper positive charge layer (upper red markers) is located above 11 km and extends to

approximately 15 km. The mid-level negative charge region (see mid-level blue markers) is located between 5 km and 9 km, whereas the lower positive charge region is identified below 5 km altitude. It is worth mentioning that the detection of electrical breakdown above the upper positive charge region suggests the presence of a negative screening layer, located at an altitude between 15 km and 16 km, as shown by the upper blue markers in Fig. 7. In the same figure, the locations of initiation of each flash, defined as the location of the first LMA source, are labeled. Initiations of flashes were located between 9 km and 11.4 km height in a quasi-neutral charge region between the upper positive and mid-level main negative charge layers.

3.4. Sferics

In the previous sections we have shown that the lightning flashes initiated with strong VHF emissions and blue optical luminosity. These features suggest that the initiations are related to fast breakdown that may generate NBEs sferics. To confirm the presence of NBEs, we analyzed the related magnetic field sferic waveforms. Fig. 8 presents the four magnetic field waveforms (5–200 kHz) at the time of the initiation of the flashes. In the first three flashes (Fig. 8a-c), the magnetic field signatures show isolated bipolar waveforms with durations between 20 and 30 μs confirming the NBE nature of the events. Assuming that the source region of the magnetic field signals is at the location of the first LMA source, we correct the transit time from the source to the receiver (~20 km) assuming a wave propagation at the speed of light. In flashes 1–3, the sferic was produced about 25 μs after the first VHF source (asterisk makers). The onset time of the magnetic field matches with the detection of LINET in the first flash (Fig. 8a) and with the GLD360 detection in the second flash (Fig. 8b). In the fourth flash, the magnetic field shows a more complex waveform (Fig. 8d). In this case, a small isolated bipolar pulse occurred about 300 μs before the first detected VHF source. At the time of the VHF source the magnetic field presents a more complex waveform that lasts for about 120 μs.

When the radio signals are compared with the optical radiation detected by ASIM, it is necessary to take into account the time uncertainties resulting from several factors. The first one is due to the uncertainty of the ASIM absolute time accuracy which is assumed to be about a few tens of ms with respect to the GPS time (Heumesser et al., 2021). This uncertainty can be reduced by correcting the time by identifying the same optical pulses detected by GLM and ISS-LIS. With this method, the uncertainty can be reduced at the order of 1–2 ms. In addition to the absolute time accuracy, there is the influence of the light scattering and absorption in the cloud plus the transit time to reach the ISS. Taking these factors into account, the shaded areas in Fig. 8 indicate the range of the UT time uncertainty of the blue luminosity signals. In the first three flashes, the blue luminosity starts simultaneously with the VHF and VLF/LF emissions. This seems to not be the case in the fourth

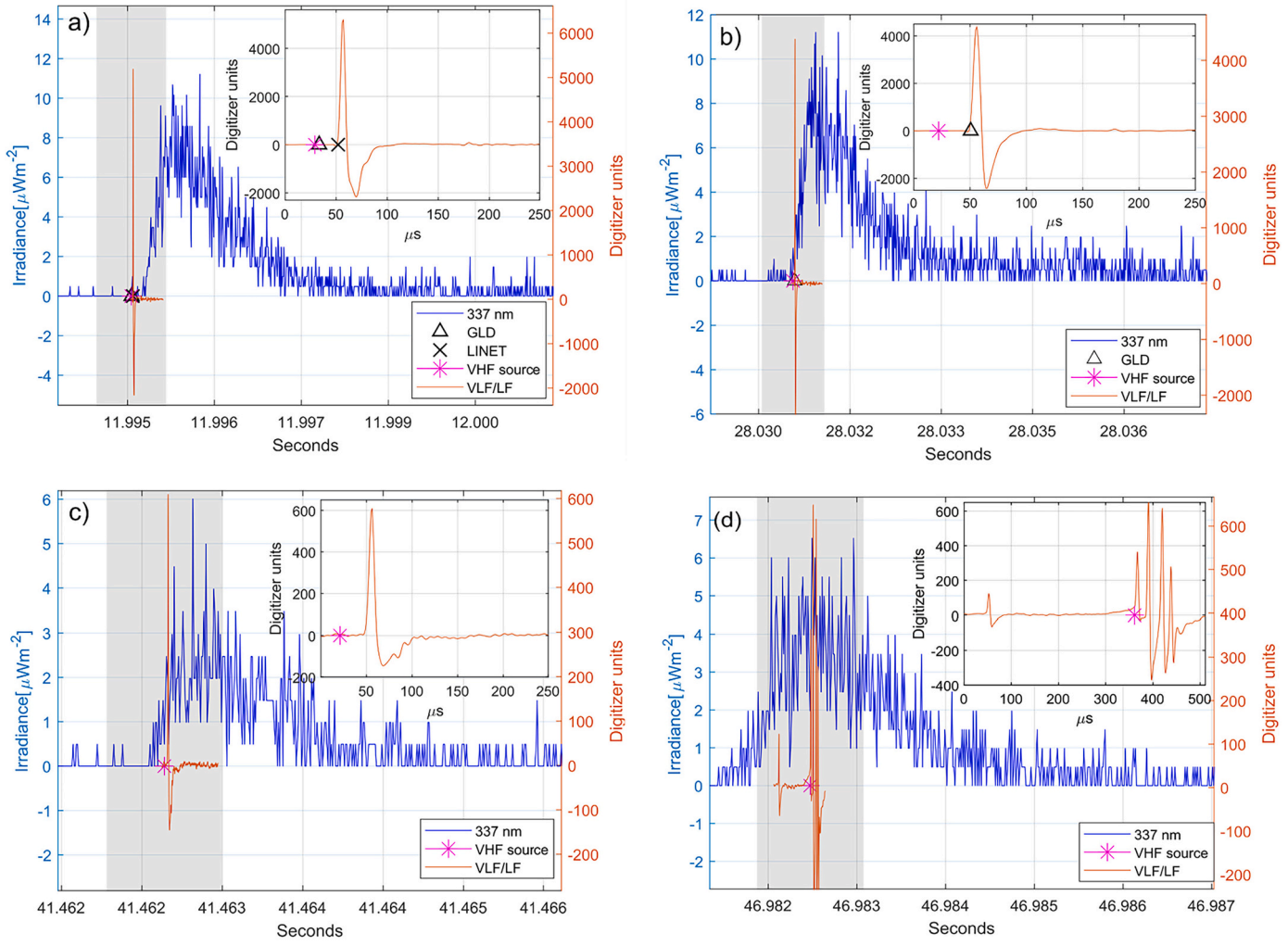

Fig. 8. VLF/LF waveforms and blue optical emissions during the initiation of each flash. Panels (a) corresponds to the first flash occurred at 06:05:11, (b) to the second flash at 06:05:28, (c) to the third flash at 06:05:41 and (d) to the fourth flash at 06:05:46. The shadow area corresponds to the range of time uncertainty of the optical signals. (For interpretation of the references to colour in this figure legend, the reader is referred to the web version of this article.)

flash where a small bipolar magnetic field pulse is located at the rise time of the blue luminosity and the first VHF source at the peak of the blue. At the peak of the blue emission, the magnetic field signal presents a complex waveform. The VHF power at the initiation of this flash was low (20 dBW) compared to the other three flashes. It is important to remark that in all the four cases (Fig. 8), the blue signals can shift in time within the marked uncertainty ranges (shaded areas).

4. Discussion

In the previous section the optical, VHF and sferics properties of the four initiations of the lightning flashes have been described. These flashes occurred within 1 min and clustered in distance within 5 km. These space-time cluster characteristics have been already reported by e.g.: Tilles et al. (2019) and Stanley et al. (2018) showing short periods of high rates of NBE (e.g. ~40 NBEs within 1 min). The proximity in space and time of each flash initiation suggests that the charge removed by each flash, including the NBE, is not enough to suppress the conditions of new initiation of fast breakdown. Alternatively, the thundercloud charging mechanisms or the redistribution of charge within the clouds at these locations may be very effective during this period.

The initiation of the flashes one and two exhibited typical features of fast breakdown: radiation bursts of high VHF power (>100 kW) simultaneously with intense bipolar VLF/LF sferics (NBEs) (Smith et al., 2004; Wu et al., 2012; Rison et al., 2016; Tilles et al., 2019). Assuming their locations are those of the first LMA sources, the NBEs initiated between the midlevel negative and the upper positive electrical charge regions (markers 1 and 2 in Fig. 7). In both flashes, the direction of the currents of the NBE, derived from the components of the magnetic fields (not shown in Fig. 8), were pointing downwards. Rison et al. (2016) and Tilles et al. (2019) already noticed the existence of a weaker version of the fast breakdown in terms of LMA VHF power and associated sferic amplitudes. In the case of the third flash, the LMA VHF power at initiation was one order of magnitude lower than in the first two flashes (Table 1), but was also accompanied by VLF/LF radio bipolar emission and dominant blue luminosity. The direction of the current derived from the magnetic field components as well as the source location was similar to flashes 1 and 2. In the case of the fourth flash, although initiated with a blue pulse that might indicate the occurrence of fast breakdown, we cannot accurately determine the direction of the current because of the complex magnetic field signals at the time of the VHF source.

The coincidence in time (Fig. 8a-c) between the blue luminosity and the fast breakdown, with the absence of red emissions, is consistent with the non-thermal discharge nature of the FPB and the FNB as it was previously proposed by Rison et al. (2016), Liu et al. (2019) and Tilles et al. (2019). In Fig. 8a-c, the onset of the blue emission likely corresponds to the time of occurrence of the fast breakdown. The presence of isolated 337 nm emissions is associated with corona streamer discharges occurring inside thunderclouds as recently proposed by Soler et al. (2020) using ASIM measurements. Following Soler et al. (2020) and Luque et al. (2020), the temporal dependence of optical emissions from the interior of thunderclouds is controlled by the time scale of multiple photon scattering by cloud droplets and ice crystals (e.g. Thomson and Krider, 1982; Light et al., 2001). Under the assumptions that the optical pulse is impulsive and localized, that the cloud is homogeneous and bounded above by a plane, and that the photons exit the cloud isotropically, with scattering outside the cloud being negligible, one can derive a simple expression for the signal registered by a photometer above the cloud top (see Appendix A). So, from the measured blue pulses, the depth of the emission source within the cloud can be estimated as done in Appendix A. The average altitude of the luminosity source for the first two flashes is included in Table 1. The obtained altitudes from the optical signals (10.5 km and 11 km for flashes one and two, respectively) agree with the altitudes of the first LMA sources (11.2 km and 11 km, respectively). This concurrence supports that the source of the dominant blue optical emission is from non-thermal discharges of the fast breakdown. Unfortunately, the optical pulses of the third and fourth flashes do not allow a good estimation of the depth, as discussed in Appendix A.

From the summary in Table 1, we found that there is not a simple relation between the amplitude of the blue radiance with the VHF power or the peak of the magnetic field. However, the first two flashes produced higher amplitudes of blue irradiance, VHF power, and LF/VLF magnetic fields compared with the flashes three and four. In the third flash, the higher altitude would lead to increased luminosity, but this is not observed, suggesting that the optical emission is more related to the 'intensity' of the fast breakdown. Rison et al. (2016) and Tilles et al. (2019) already noticed the existence of a weaker version of the fast breakdown in terms of LMA VHF power and associated sferic amplitude. Here we have shown that the weak fast breakdown events also produced comparable optical radiance to the strong ones. From Table 1 we find some proportionality between the levels of VHF radio frequency power and the peak of the magnetic field. This relation is in good agreement with Liu et al. (2019) who theoretically showed the dependence of the amplitudes in the VLF to VHF radio spectrum on the number of streamers. But this proportionality on the levels of radio emissions is not found in the blue optical emissions. As is shown in Fig. 8, the two strong NBE in the flashes one and two produced similar peaks of radiance (~10 $\mu W/m^2$), whereas the weak NBE in the flashes three and four produced slightly lower peaks of radiance (~6 $\mu W/m^2$). In addition, there is not much difference between the peak of the radiance of the blue emission in the third flash that initiated around 11.4 km and the fourth that initiated at much lower altitude (9 km). Actually, the cloud top energy (van der Velde et al., 2020) of blue emissions of flash 4, calculated for a time interval of 2 ms, is comparable to those of flashes one and two (Fig. S5 to S8 in the supplementary material). In the case of the third flash, the cloud top energy is the lowest, although the source was assumed to be higher, as discussed before. The lack of a clear relation between the amplitude of the blue luminosity and the strength of the fast breakdown, characterized by radio wave emissions, may suggest a dependence of the photon flux at the detector on the vertical and horizontal extent of the source, and of spatial inhomogeneities of the cloud properties.

5. Conclusions

In this paper we presented four simultaneous observations with a ground-based LMA and from space by ASIM-MMIA of fast breakdown processes that occurred at the initiation of four lightning flashes. Two of

Table 1
Summary of the properties of the investigated flash initiations.

Flash	LMA power (kW)	LMA initiation (km)	Peak blue radiance ($\mu W/m^2$)	Rise time blue (μs)	Duration blue (ms)	Peak blue cloud top energy** (J)	Peak red cloud top energy** (J)	Altitude of blue emission* (km)	Peak magnetic field (d.u.)
1	178	11.2	10.6	380	2.3	3240	–	10.5	5003
2	269	11.0	10.3	200	3	2306	–	11.3	4410
3	10	11.4	6	500	1.8	828	–	–	601
4	0.1	9	6.5	390	2	2480	324	–	120

* Average altitudes calculated in Appendix A.
** Cloud top optical energies are included in the supplementary material.

the events presented clear features of strong fast breakdown characteristics: very high VHF power (>100 kW) and bipolar magnetic fields (NBE). Three of the events were identified to be fast positive breakdown where the detected blue luminosity was not accompanied by red optical emissions. The findings of this study can be summarized as follows:

1. The detection of blue luminosity without red optical emissions at the flash initiations with the occurrence of high VHF power and NBE confirms the streamer nature of the fast breakdown (Rison et al., 2016)
2. Despite the significant differences in the amplitudes of the VHF power and the sferics between the 'strong' and 'weak' NBEs the amplitude of the blue radiance did not change accordingly.
3. The proportionality between the amplitudes in the VHF power and the magnetic field of the sferics supports that these are highly dependent on the number of streamers (Liu et al., 2019).
4. The lack of proportionality between the value of the radio emissions and the optical blue luminosity needs further investigation.

Declaration of Competing Interest

The authors declare that they have no known competing financial interests or personal relationships that could have appeared to influence the work reported in this paper.

Acknowledgments

The UPC contribution: This work was supported by research Grants ESP2013-48032-C5-3-R, ESP2015-69909-C5-5-R and ESP2017-86263-C4-2-R funded by MCIN/AEI/ 10.13039/501100011033 and by "ERDF A way of making Europe", by the "European Union"; and Grant PID2019-109269RB-C42 funded by MCIN/AEI/ 10.13039/501100011033.

The IAA contribution: This work was supported by the Spanish Ministry of Science and Innovation, Ministerio de Ciencia e Innovación (AEI) under project PID2019-109269RB-C43 and the FEDER program. FJPI acknowledges the sponsorship provided by the Federal Ministry for Education and Research of Germany through the Alexander von Humboldt Foundation. AL was supported by the European Research Council (ERC) under European Union Horizon 2020 Framework Programme/ ERC Grant Agreement 681257. Authors FJGV, FJPI, and AL acknowledge financial support from the State Agency for Research of the Spanish MCIU through the "Center of Excellence Severo Ochoa" award for the Instituto de Astrofísica de Andalucía (SEV- 2017-0709). The UV contribution: This work was supported by research grants from the Spanish Ministry of Economy and the European Regional Development Fund (FEDER): ESP2013-48032-C5-1-R, ESP2015-69909-C5-1-R and ESP2017-86263-C4-1-R. The UB (University of Bergen) would like to thank the Research Council of Norway under contracts 223252/F50 (CoE). The USP (University of Sao Paulo) contribution: This work was supported by Coordenação de Aperfeiçoamento de Pessoal de Nível Superior (CAPES)— Print Project (grant number: 88887.370081/2019-00). ASIM is a mission of The European Space Agency (ESA). The project is funded by ESA and by national grants of Denmark, Norway, and Spain. We thank Keraunos(Colombia) for the LINET data

Appendix A

The equation below describes the light pulse shape observed above a cloud and provides a rough estimate of event depths (with respect to cloud top) inside thunderclouds (Soler et al., 2020; Luque et al., 2020).

$$f(t) = \frac{\theta(t-t_0)e^{2\sqrt{\nu\tau}}}{\tau\sqrt{\pi}}\left(\frac{\tau}{t-t_0}\right)e^{-\tau(t-t_0)-\nu(t-t_0)}, \text{with} \int_{-\infty}^{+\infty} f(t)dt = 1 \quad (A.1)$$

where θ is the step function, t_0 is the emission time, and $\tau = L^2/4D$ is the characteristic time of the process. Given a photometer signal, one can fit it to Eq. (A.1) and obtain values for the parameters t_0, τ, and ν. Then the depth of the event can be estimated as $L = (4D\tau)^{1/2} \approx (4\Lambda c\tau/(3(1-g)))^{1/2}$. In this work we used g = 0.87 (Thomson and Krider, 1982) and, since the radius of the cloud droplets is much larger than the optical wavelengths involved, the photon mean free path $\Lambda = (2\pi r^2 n)^{-1} = 4$ m to 16 m, corresponding to a scatterer concentration $n = 10^8$ m^{-3} and radii r = 10 to 20 μm (Thomson and Krider, 1982), which correspond to a range of the diffusion coefficient $D = \Lambda c/(3(1-g\omega_0))$ (Koshak et al., 1994), from 3×10^9 to 12×10^9 m^2 s^{-1}, and where g is the scattering asymmetry parameter, and ω_0 (close to one under our conditions) is the single-scattering albedo that indicates the probability that a photon is reemitted after a scattering event. A cloud top height of 15 km of the thunderstorm is considered. We have fit Eq. (A.1) to the isolated 337.0 nm pulses associated to the first two flashes (06:05:11 and 06:05:28) in order to derive their emission depth in the cloud. Unfortunately, the shapes of the blue pulses in the flashes three and four (06:05:41 and 06:05:46) did not allow a good fit. The obtained ranges are indicated in Table A1.

Table A1
Estimated height of the blue source emission in the cloud. The cloud top is assumed to be at 15 km.

Flash	Height
1	9–12 km
2	10–12.5 km
3	–
4	–

Appendix B. Supplementary data

Supplementary data to this article can be found online at https://doi.org/10.1016/j.atmosres.2021.105981.

References

Aranguren, D., López, J., Inampués, J., Torres, H., Betz, H., 2017. Cloud-to-ground lightning activity in Colombia and the influence of topography. J. Atmos. Sol. Terr. Phys. https://doi.org/10.1016/j.jastp.2016.08.010.

Bandara, S., Marshall, T., Karunarathne, S., Stolzenburg, M., 2020. Electric field change and VHF waveforms of positive Narrow Bipolar events in Mississippi thunderstorms. Atmos. Res. 243 (2020) https://doi.org/10.1016/j.atmosres.2020.105000.

Bazelyan, E.M., Raizer, Y.P., 1997. Spark Discharge, Chap. 1. Routledge, pp. 8–12 (CRC Press. ISBN 9780849328688).

Betz, H., Schmidt, K., Oettinger, W., 2009. LINET—An international VLF/LF lightning detection network in Europe. In: Lightning: Principles, Instruments and Applications, Chap. 5. Springer, Germany, pp. 115–140. https://doi.org/10.1007/978-1-4020-9079-0_5.

Blakeslee, R.J., Lang, T.J., Koshak, W.J., Buechler, D., Gatlin, P., Mach, D.M., Stano, G.T., Virts, K.S., Walker, T.D., Cecil, D.J., Ellett, W., Goodman, S.J., Harrison, S., Hawkins, D.L., Heumesser, M., Lin, H., Maskey, M., Schultz, C.J., Stewart, M., Bateman, M., Chanrion, O., Christian, H., 2020. Three years of the lightning imaging sensor onboard the international space station: expanded global coverage and enhanced applications. J. Geophys. Res. Atmos. 125 https://doi.org/10.1029/2020JD032918 e2020JD032918.

Chanrion, O., Neubert, T., Lundgaard Rasmussen, I., Stoltze, C., Tcherniak, D., Jessen, N. C., Polny, J., Brauer, P., Balling, J.E., Savstrup Kristensen, S., Forchhammer, S., Hofmeyer, P., Davidsen, P., Mikkelsen, O., Bo Hansen, D., Bhanderi, D.D.V., Petersen, C.G., Lorenzen, M., 2019. The Modular Multispectral Imaging Array (MMIA) of the ASIM Payload on the International Space Station. Space Sci. Rev. 215 (4) https://doi.org/10.1007/s11214-019-0593-y.

Eack, K.B., 2004. Electrical characteristics of narrow bipolar events. Geophys. Res. Lett. 31 (20) https://doi.org/10.1029/2004GL021117.

Goodman, S., Blakeslee, R., Koshak, W., 2008. Geostationary lightning mapper for GOES-R. NOAA/NESDIS/Center for Satellite Applications and Research WW707, 2–63.

Goodman, S.J., Blakeslee, R.J., Koshak, W.J., Mach, D., Bailey, J., Buechler, D., Carey, L., Schultz, C., Bateman, M., McCaul, E., Stano, G., 2013. The GOES-R Geostationary Lightning Mapper (GLM). Atmos. Res. https://doi.org/10.1016/j.atmosres.2013.01.006.

Heumesser, M., Chanrion, O., Neubert, T., Christian, H.J., Dimitriadou, K., Gordillo-Vazquez, F.J., et al., 2021. Spectral observations of optical emissions associated with Terrestrial Gamma-Ray Flashes. Geophys. Res. Lett. 48 https://doi.org/10.1029/2020GL090700 e2020GL090700.

Jacobson, A.R., Light, T.E.L., Hamlin, T., Nemzek, R., 2013. Joint radio and optical observations of the most radio-powerful intracloud lightning discharges. Ann. Geophys. 31 (3) https://doi.org/10.5194/angeo-31-563-2013.

Kolmašová, I., Santolík, O., Defer, E., Rison, W., Coquillat, S., Pedeboy, S., Lán, R., Uhlíř, L., Lambert, D., Pinty, J.P., Prieur, S., Pont, V., 2018. Lightning initiation: strong pulses of VHF radiation accompany preliminary breakdown. Sci. Rep. 8 (1) https://doi.org/10.1038/s41598-018-21972-z.

Koshak, W.J., Solakiewicz, R.J., Phanord, D.D., Blakeslee, R.J., 1994. Diffusion model for lightning radiative transfer. J. Geophys. Res. 99 (D7), 14361–14371. https://doi.org/10.1029/94JD00022.

Le Vine, D.M., 1980. Sources of the strongest RF radiation from lightning. J. Geophys. Res. 85 (C7) https://doi.org/10.1029/jc085ic07p04091.

Light, T.E., Suszcynsky, D.M., Kirkland, M.W., Jacobson, A.R., 2001. Simulations of lightning optical waveforms as seen through clouds by satellites. J. Geophys. Res. 106 (D7) https://doi.org/10.1029/2001JD900051, 17,103–17,114.

Liu, N., Dwyer, J.R., Tilles, J.N., Stanley, M.A., Krehbiel, P.R., Rison, W., Brown, R.G., Wilson, J.G., 2019. Understanding the Radio Spectrum of Thunderstorm Narrow Bipolar events. J. Geophys. Res.-Atmos. https://doi.org/10.1029/2019JD030439.

López, J.A., Montanyà, J., van der Velde, O.A., Pineda, N., Salvador, A., Romero, D., Aranguren, D., Taborda, J., 2019. Charge structure of two tropical thunderstorms in Colombia. J. Geophys. Res.-Atmos. https://doi.org/10.1029/2018JD029188.

Lu, G., Cummer, S.A., Lyons, W.A., Krehbiel, P.R., Li, J., Rison, W., Thomas, R.J., Edens, H.E., Stanley, M.A., Beasley, W., MacGorman, D.R., Van Der Velde, O.A., Cohen, M.B., Lang, T.J., Rutledge, S.A., 2011. Lightning development associated with two negative gigantic jets. Geophys. Res. Lett. https://doi.org/10.1029/2011GL047662.

Luque, A., Gordillo-Vázquez, F.J., Li, D., Malagón-Romero, A., Pérez-Invernón, F.J., Schmalzried, A., et al., 2020. Modeling lightning observations from space-based platforms (CloudScat. jl 1.0). Geosci. Model Dev. Discuss. 13, 1–26.

Lyu, F., Cummer, S.A., Qin, Z., Chen, M., 2019. Lightning Initiation Processes Imaged with very High Frequency Broadband Interferometry. J. Geophys. Res.-Atmos. 124 (6) https://doi.org/10.1029/2018JD029817.

Marshall, T., Bandara, S., Karunarathne, N., Karunarathne, S., Kolmasova, I., Siedlecki, R., Stolzenburg, M., 2019. A study of lightning flash initiation prior to the first initial breakdown pulse. Atmos. Res. 217 https://doi.org/10.1016/j.atmosres.2018.10.013.

Neubert, T., Østgaard, N., Reglero, V., et al., 2019. The ASIM Mission on the International Space Station. Space Sci. Rev. 215, 26. https://doi.org/10.1007/s11214-019-0592-z.

Rison, W., Thomas, R., Krehbiel, P., Hamlin, T., Harlin, J., 1999. A GPS-based three-dimensional lightning mapping system: initial observations in Central New Mexico. Geophys. Res. Lett. 26 (23), 3573–3576. https://doi.org/10.1029/1999GL010856.

Rison, W., Krehbiel, P.R., Stock, M.G., Edens, H.E., Shao, X.M., Thomas, R.J., Stanley, M. A., Zhang, Y., 2016. Observations of narrow bipolar events reveal how lightning is initiated in thunderstorms. Nat. Commun. https://doi.org/10.1038/ncomms10721.

Said, R.K., Cohen, M.B., Inan, U.S., 2013. Highly intense lightning over the oceans: estimated peak currents from global GLD360 observations. J. Geophys. Res. Atmos. 118, 6905–6915. https://doi.org/10.1002/jgrd.50508.

Smith, D.A., Heavner, M.J., Jacobson, A.R., Shao, X.M., Massey, R.S., Sheldon, R.J., Wiens, K.C., 2004. A method for determining intracloud lightning and ionospheric heights from VLF/LF electric field records. Radio Sci. 39, RS1010. https://doi.org/10.1029/2002RS002790.

Soler, S., Pérez-Invernón, F.J., Gordillo-Vázquez, F.J., Luque, A., Li, D., Malagón-Romero, A., Neubert, T., Chanrion, O., Reglero, V., Navarro-González, J., Lu, G., Zhang, H., Huang, A., Østgaard, N., 2020. Blue optical observations of narrow bipolar event by ASIM suggest corona streamer activity in thunderstorms. J. Geophys. Res.-Atmos. 125 https://doi.org/10.1029/2020JD032708 e2020JD032708.

Soler, S., Gordillo-Vázquez, F.J., Pérez-Invernón, F.J., Luque, A., Li, D., Neubert, T., Chanrion, O., Reglero, V., Navarro-González, J., Ostgaard, N., 2021. Global frequency and geographical distribution of nighttime streamer corona discharges (BLUEs) in thunderclouds. Geophys. Res. Lett. 48 https://doi.org/10.1029/2021GL094657.

Stanley, M.A., Rison, W., Tilles, J.N., Krehbiel, P.R., Brown, R.G., Wilson, J.G., Liu, N.Y., 2018. Broadband VHF interferometry within the Kennedy Space Center lightning mapping array. In: In 25th International Lightning Detection Conference (ILDC) and 7th International Lightning Meteorology Conference (ILMC). Ft. Lauderdale, Florida..

Thomas, R., Krehbiel, P., Rison, W., Hunyady, S., Winn, W., Hamlin, T., Harlin, J., 2004. Accuracy of the lightning mapping array. J. Geophys. Res. 109, D14207. https://doi.org/10.1029/2004JD004549.

Thomson, L.W., Krider, E.P., 1982. The Effects of Clouds on the Light Produced by Lightning. J. Atmos. Sci. 39 (9) https://doi.org/10.1175/1520-0469(1982)039<2051:TEOCOT>2.0.CO;2.

Tilles, J.N., Liu, N., Stanley, M.A., Krehbiel, P.R., Rison, W., Stock, M.G., Dwyer, J.R., Brown, R., Wilson, J., 2019. Fast negative breakdown in thunderstorms. Nat. Commun. 10 (1) https://doi.org/10.1038/s41467-019-09621-z.

Tilles, J.N., Krehbiel, P.R., Stanley, M.A., Rison, W., Liu, N., Lyu, F., et al., 2020. Radio interferometer observations of an energetic in-cloud pulse reveal large currents generated by relativistic discharges. J. Geophys. Res.-Atmos. 125 https://doi.org/10.1029/2020JD032603 e2020JD032603.

van der Velde, O.A., Montanyà, J., 2013. Asymmetries in bidirectional leader development of lightning flashes. J. Geophys. Res.-Atmos. 118, 13,504–13,519. https://doi.org/10.1002/2013JD020257.

van der Velde, O.A., Montanyà, J., Neubert, T., Chanrion, O., Østgaard, N., Goodman, S., et al., 2020. Comparison of high-speed optical observations of a lightning flash from space and the ground. Earth Space Sci. 7 https://doi.org/10.1029/2020EA001249 e2020EA001249.

Wu, T., Dong, W., Zhang, Y., Funaki, T., Yoshida, S., Morimoto, T., Ushio, T., Kawasaki, Z., 2012. Discharge height of lightning narrow bipolar events. J. Geophys. Res. 117, D05119. https://doi.org/10.1029/2011JD017054.